

Supplement of Atmos. Chem. Phys., 20, 1075–1087, 2020  
<https://doi.org/10.5194/acp-20-1075-2020-supplement>  
© Author(s) 2020. This work is distributed under  
the Creative Commons Attribution 4.0 License.



*Supplement of*

## **Cloud history can change water–ice–surface interactions of oxide mineral aerosols: a case study on silica**

**Ahmed Abdelmonem et al.**

*Correspondence to:* Ahmed Abdelmonem (ahmed.abdelmonem@kit.edu)

The copyright of individual parts of the supplement might differ from the CC BY 4.0 License.

## S1 Thermodynamic considerations

Calculations have been done using and data pertaining to silica (Marion et al., 2009) combined with the the frezchem database included in PHREEQC Interactive, version 3.4.0.12927 (released November 9, 2017). The calculations were done for the experimental conditions at room temperature in terms of solution composition. Two extreme cases were considered:

5 Ice formation and no ice formation. When including the formation of ice, super-cooling cannot be simulated. In this case the pH drops in the H<sub>2</sub>O fraction that is not freezing because the solutes are concentrated in liquid that remains due to the freezing point depression. Since in the experiments in no case all of the water freezes, the calculations overestimate the effect. The final calculated volume of liquid water at -40 °C is about 300 μL, which contains all the solutes. In this case the pH drops to about -1.4. In our experiments, the freezing and melting is occurring at the surface. So extreme conditions could  
10 occur during the melting only, when remaining solution connects to the interfacial water film, but as pointed out above in all cycles much larger volumes of liquid water are expected compared to the 300 μL noted above. The amount of dissolved silica as a function of the temperature at equilibrium is shown in Figure S1 as a dotted line. The equilibrium concentration of silica at -40°C is about 100 μM based on the available thermodynamic data.

When excluding the formation of ice in the calculation as the other extreme, the water remains liquid and slightly changes its  
15 volume, which affects molar concentrations accordingly. The pH remains more or less constant in this case. The concentration of silica at -40°C is about 410 μM, i.e. a factor 4 higher than in the previous case. This is due to the higher salt concentration in the previous example, where the activity coefficients of the solutes cause a decrease in the solubility.

The measured concentration of silica in the experiments was about 41 μM.

The measurements and observations can be related to the above calculations as follows:

- 20 - The measured silica concentration (at the end of the experiment at TP cycle 25) is below any of the estimates for equilibrium solubility for the conditions of our experiments. This means that there is a driving force for further dissolution. This corroborates that the number of cycles is the major factor and not the time of exposure, since the prolonged time of exposure at room temperature (i.e. TP > 25) should have caused more dissolution and thus more SHG enhancement. Instead the freeze/melt cycles cause the changes in SHG with lowering temperature.
- 25 - The lower silica solubility, with decreasing temperature, should favor the interaction of dissolved silica with the fused silica surface. Based on the work by (Schaefer et al., 2018), this corroborates the idea that there is a trend to silica adsorption with the decreased temperature. There is ample information for example that dissolved Al adsorbs to aluminium oxide and our experiments with dissolved silica in the presence of fused silica also shows such interaction, so that the temperature dependence in terms of silica solubility would corroborate our interpretation in  
30 the main text.

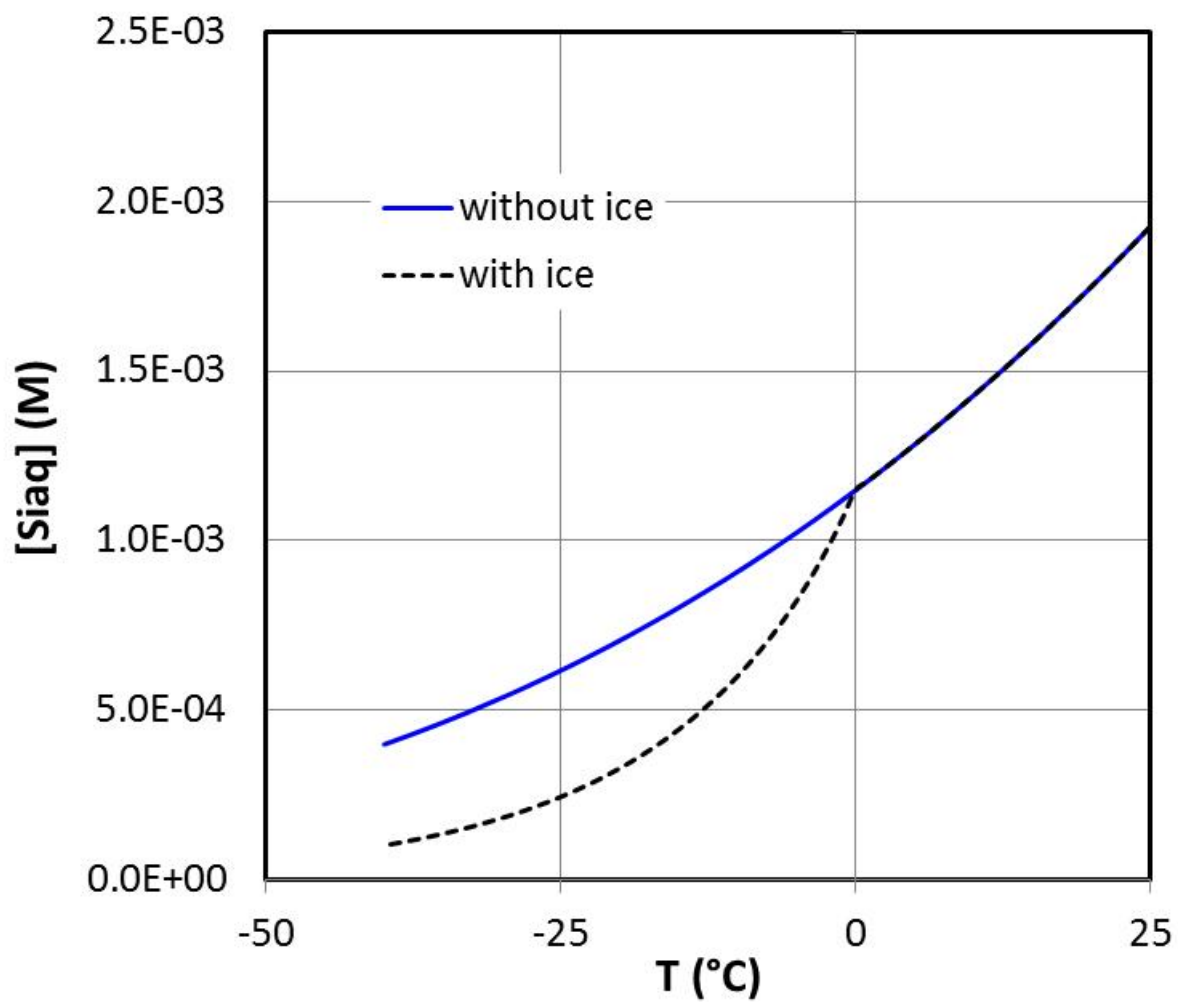
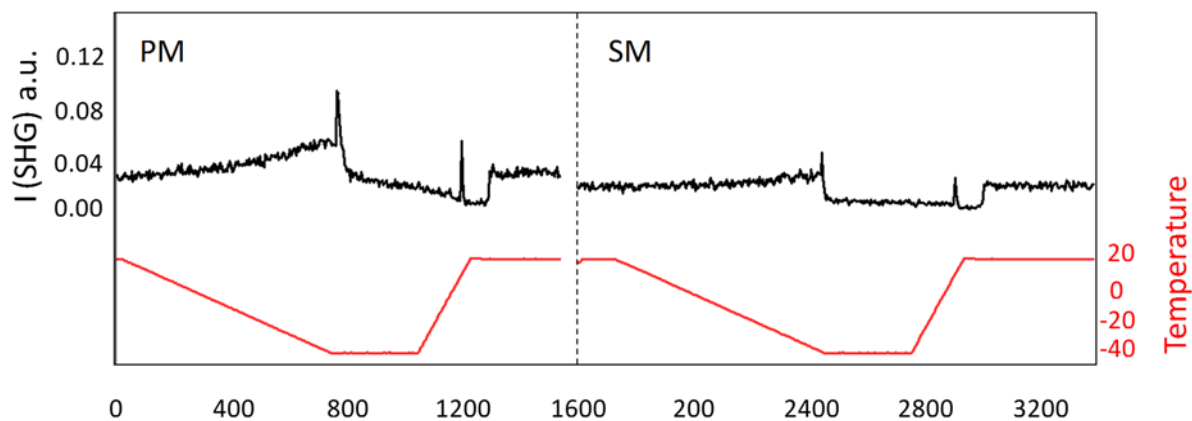


Figure S1: Evolution of dissolved silica in a solution of 1 mM HCl (pH 3 at room temperature) with decreasing temperature in the presence of ice formation (dotted line) and without ice forming (full line). Calculations were done as specified in the text.

## S2 Comparison between PM and SM polarization combinations under the geometrical conditions of the used SHG setup



- 5 Figure S2: SHG signal (rescaled raw data) at the aged pH3 solution-silica interface as a function of time/temperature for two successive TP cycles with different beam polarization combinations (PM: P-polarized SHG / 45°-polarized incident, and SM: S-polarized SHG / 45°-polarized incident) incident with an angle close to the critical angle of total internal reflection. An aged sample was used to minimize the sample surface change during the two runs. The data show that the signal versus temperature for both polarization combinations behaves identically.

### S3 SHG vs. Cycle number during cooling at different temperatures

Fig 4c in the manuscript looks identical to 4b. It is our intention to show that at the onset point, Fig 4c, there is nothing exceptional happens although the onset temperatures are different.

In Fig. S3 we show the change in signal with aging at other temperatures. Since the paper discusses the restructuring of water upon cooling and relates this to the freezing process, we select here a set of temperatures during cooling to plot the signal as a function of cycle number. Figure S3 shows the averaged SHG liquid signal as a function of TP cycle number at five different temperatures on the cooling path. The minimum points occur at lower cycle numbers for lower temperatures (summarized in table S1). The closest cycle number to the liquid signal minimum decreases with temperature. This assists our conclusion that cooling favors the uptake of dissolved silica (i.e. adsorption).

Time with respect to scan start (s)	Temperature (°C)	Closest cycle no. to minimum signal
a) 0 sec	20	7
b) 120 sec	10	6
c) 240 sec	0	5
d) 480 sec	-20	4
e) 630 sec	-32	3

Table S1: The selected temperatures in Figure S3 and the corresponding TP cycle number of minimum SHG liquid signal.

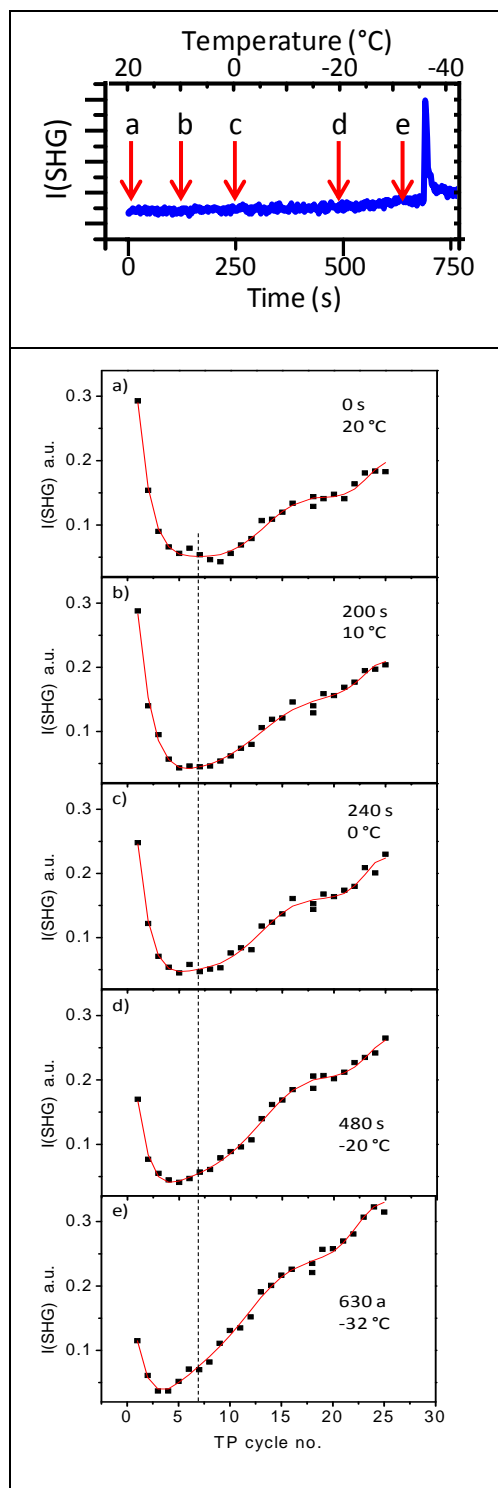
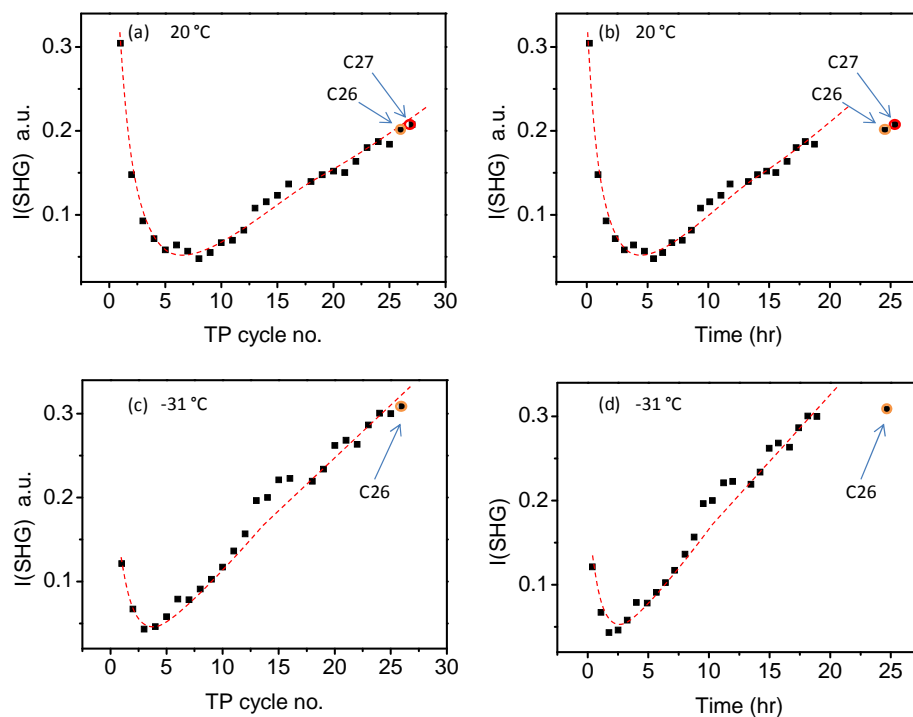


Figure S3: Upper panel: a sample plot of SHG vs. cycle number during cooling. Lower panel: The averaged SHG liquid signal as a function of TP cycle number at five different temperatures during cooling before freezing. The red lines on the plots are guiding lines through the data points.

#### S4 The observed fast aging, is it a matter of time only?



5 Figure S4: SHG signal at pH3 solution-silica interface as a function of TP cycle number (a) and time (b) of liquid signal at 20 °C during repeating the freezing-melting TP. The dashed red lines are trend lines. CS26 and CS27 denote data points that lie on the trend line in (a) but not in (b). This shows that the significant aging we observe in this work arises from the freezing-melting process and not from the time the sample being in contact with solution. Furthermore, as discussed in section S1, the measured silica concentration should favor further dissolution at room temperature, but this does not explain the SHG data.

S5 SHG versus pH for our Si sample used in this work

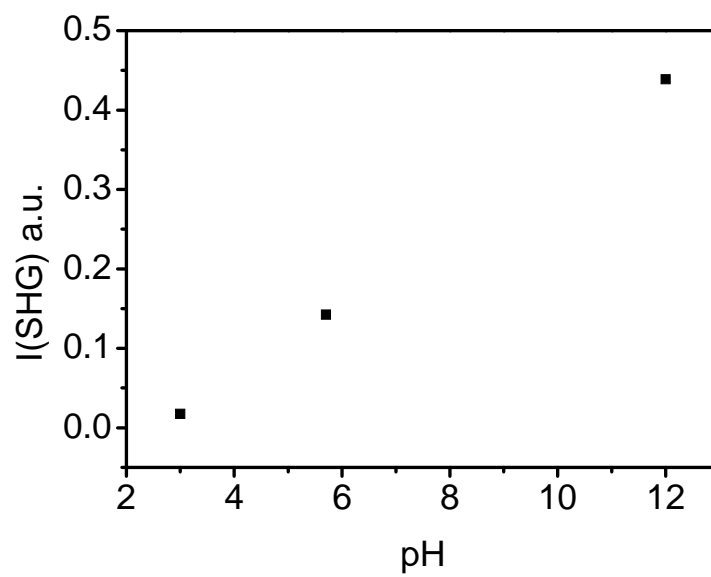
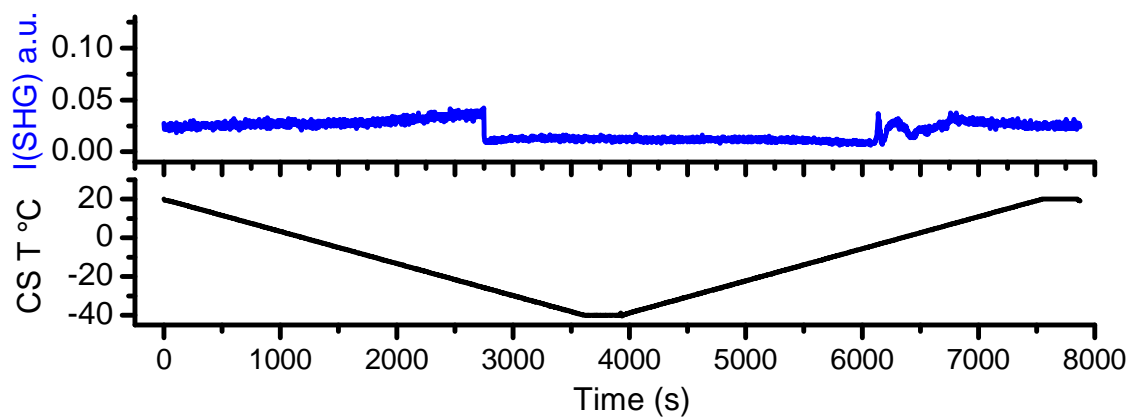


Figure S5: SHG signal as a function of pH for our fresh sample (before aging) at 20 °C.

## S6 Slow TP



5 Figure S6: SHG signal at pH3 solution-silica interface as a function of time for the C27 run which was carried out at cooling and heating rates ( $= 1 \text{ }^\circ\text{C} / \text{min}$ ) slower than the standard TP.



## S7 Top view of the measuring cell with partially frozen water

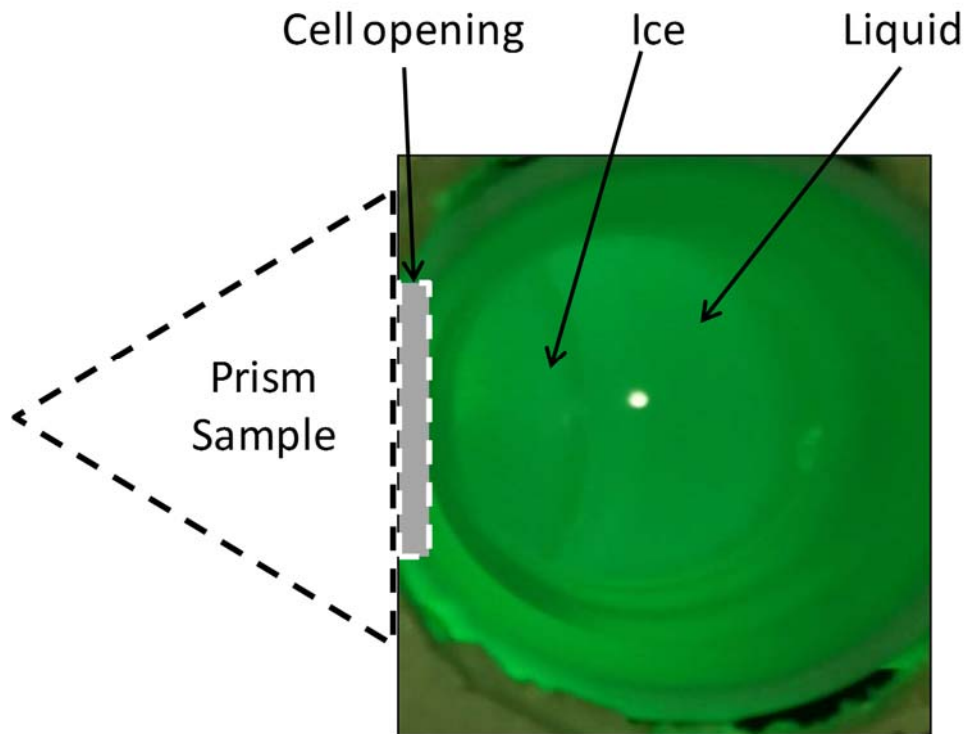


Figure S7: Photo (top view) of the bulk ice formed after freezing and waiting for 5 min at  $-40\text{ }^{\circ}\text{C}$ . The freezing starts at the surface of the sample and grows at the expense of water on the other side. The size of the bulk ice is proportional to the time of keeping the system supercooled after the freezing event. The ice piece is stuck in the cell opening and the process of melting and departing from the sample neighborhood depends on the cell geometry and bulk ice size as well as the thermal conditions. All these parameters affect the appearance and disappearance of the confined liquid signal.

5

## References

- 10 Marion, G. M., Crowley, J. K., Thomson, B. J., Kargel, J. S., Bridges, N. T., Hook, S. J., Baldrige, A., Brown, A. J., Ribeiro da Luz, B., and de Souza Filho, C. R.: Modeling aluminum–silicon chemistries and application to Australian acidic playa lakes as analogues for Mars, *Geochimica et Cosmochimica Acta*, 73, 3493-3511, doi: <https://doi.org/10.1016/j.gca.2009.03.013>, 2009.
- 15 Schaefer, J., Backus, E. H. G., and Bonn, M.: Evidence for auto-catalytic mineral dissolution from surface-specific vibrational spectroscopy, *Nat. Commun.*, 9, 3316, doi: 10.1038/s41467-018-05762-9, 2018.